

## From First-Order to Two Continuous Melting Transitions: Monte Carlo Study of a New 2D Lattice-Defect Model

W. Janke and H. Kleinert

*Institut für Theorie der Elementarteilchen, Freie Universität Berlin, Arnimallee 14, 1000 Berlin 33, Germany*

(Received 6 June 1988)

We present a Monte Carlo study of a new lattice model describing defects and their elastic interactions, including a term that accounts for rotational stiffness over a length scale  $l$ . We show that, when going from small  $l$  (as in most atomic crystals) to large  $l$  (as in many molecular crystals), the melting process changes from a single first-order to two successive Kosterlitz-Thouless transitions.

PACS numbers: 64.70.Dv

The Kosterlitz-Thouless-Halperin-Nelson-Young suggestion<sup>1</sup> that two-dimensional melting should proceed via two successive continuous transitions of the Kosterlitz-Thouless type seems to be applicable only to layers of liquid crystals.<sup>2</sup> Experiments on atomic layers loosely absorbed on surfaces,<sup>3</sup> or molecular-dynamic simulations of two-dimensional Lennard-Jones systems,<sup>4</sup> have always been found to undergo only a single first-order melting transition. For high coverage, it may sometimes become continuous,<sup>5</sup> but it has never been seen to split into two successive transitions. The same has been found for all lattice models which simulate an ensemble of crystal defects with long-range elastic interactions of linear elasticity<sup>6</sup>

$$E_{el}^{(1)} = \int d^2\xi [(\mu/4)(\partial_i u_j + \partial_j u_i)^2 + (\lambda/2)(\partial_i u_i)^2],$$

where  $u_i$  are the lattice displacements and  $\mu, \lambda$  are the elastic moduli.

Recently,<sup>7</sup> it has been shown that the characteristic parameter which specifies the difference between atomic crystals and those formed by liquid crystals, namely, the length scale of rotational stiffness,  $l$ , is responsible for the different melting processes. It appears in the second gradient elastic interaction  $E_{el}^{(2)} = 2\mu l^2 \int d^2\xi (\partial_i \omega)^2$ , where  $\omega \equiv \frac{1}{2} \epsilon_{ij} \partial_i u_j$ . If the combined energy is placed on a lattice of spacing  $a$ , with the gradients  $\partial_i$  substituted by  $1/a$  times lattice differences  $\nabla_i$  [ $\nabla_i f(\mathbf{x}) = f(\mathbf{x} + \mathbf{i}) - f(\mathbf{x})$ ], if, further, displacements  $u_i \in (-a/2, a/2)$  are scaled to  $\gamma_i = 2\pi u_i/a \in (-\pi, \pi)$  and  $\omega$  to  $\frac{1}{2} \epsilon_{ij} \nabla_i \gamma_j$ , and if discrete-valued plastic distortions are inserted to supply the Volterra jumping surfaces of dislocations and disclinations, the ensuing model energy reads (in natural units in which  $\mu a^2/4\pi^2 = 1$ , and lattice spacing  $a = 1$ )

$$E = \frac{1}{4} \sum_{\mathbf{x}, ij} (\nabla_i \gamma_j + \nabla_j \gamma_i - 4\pi n_{ij}^s)^2 + \frac{\lambda}{2\mu} \sum_{\mathbf{x}} \left[ \sum_i (\nabla_i \gamma_i - 2\pi n_{ii}^s) \right]^2 + 2l^2 \sum_{\mathbf{x}, i} \{ \nabla_i \omega - \pi [2m_i + \nabla_i (n_{12} - n_{21})] \}^2. \quad (1)$$

The partition function (with  $\beta \equiv 1/k_B T$ )

$$Z \propto \prod_{\mathbf{x}} \left( \int_{-\pi}^{\pi} d^2\gamma \right) \sum_{\{n_{ij}, m_i\}} \exp(-\beta E), \quad (2)$$

summed over all integer  $n_{ij}$  [ $n_{ij}^s \equiv (n_{ij} + n_{ji})/2$ ] and  $m_i$ , was shown<sup>7</sup> to possess, for very small  $l$ , a single first-order melting transition and, for very large  $l$ , two successive Kosterlitz-Thouless transitions (at least for  $\nu = 1$ ). A few manipulations<sup>7</sup> on the partition function lead to two alternative representations. One involves the energy [ $\bar{\nabla}_i f(\mathbf{x}) \equiv f(\mathbf{x}) - f(\mathbf{x} - \mathbf{i})$ ]

$$\beta E_r = (1/\beta) \sum_{\mathbf{x}} \left( \frac{1}{4} \{ [1/(1+\nu)] (\bar{\nabla}_i A_j)^2 - \frac{1}{2} [(1-\nu)/(1+\nu)] (\bar{\nabla}_i A_i)^2 \} + (1/8l^2) (\bar{\nabla}_k h - \epsilon_{kl} A_l)^2 \right), \quad (3)$$

with  $\nu = \lambda/(2\mu + \lambda) =$  Poisson ratio, and  $h, A_i$  being integer-valued stress gauge fields (to be summed over in the partition function). The other, dual representation is

$$\beta E_d = \beta \left\{ 4\pi^2 (1+\nu) \sum_{\mathbf{x}} \eta (\bar{\nabla} \cdot \nabla)^{-2} \eta + 4\pi^2 (2l^2) \sum_{\mathbf{x}} [\theta (-\bar{\nabla} \cdot \nabla)^{-1} \theta + \bar{\nabla}_i b_i (-\bar{\nabla} \cdot \nabla \cdot [1 - l^2 \bar{\nabla} \cdot \nabla])^{-1} \bar{\nabla}_j b_j] \right\}, \quad (4)$$

where  $b_i$  and  $\theta$  are integer-valued dislocation and disclination densities, and  $\eta = \epsilon_{ij} \nabla_i b_j + \theta$  is the so-called defect density. The partition function involving  $\beta E_r$  is a generalization of the Laplacian roughening (LR) model<sup>8</sup>  $\beta E_{LR} = [1/4\beta(1+\nu)] \sum_{\mathbf{x}} (\bar{\nabla} \cdot \nabla h)^2$  to which (3) reduces for  $l=0$  (with the associated first-order melting transition<sup>6</sup>). The other partition function generalizes the dual defect version of it,  $\beta E_{def} = \beta 4\pi^2 (1+\nu) \sum_{\mathbf{x}} \eta (\bar{\nabla} \cdot \nabla)^{-2} \eta$ , with the partition function being summed over all integer  $\eta$ . In the opposite limit of large  $l$ , at fixed  $\beta l^2$ , (3) reduces to the discrete

Gaussian (DG) model  $\beta E_{\text{DG}} = \beta^{\text{DG}} \sum_{\mathbf{x}} (\nabla h)^2$  with  $\beta^{\text{DG}} = 1/8\beta l^2$ . For  $\beta \approx 1$ , (3) becomes at  $\nu=1$

$$\beta E_{\text{DG}} = (1/8\beta) \sum_{\mathbf{x}} [A_i (-\bar{\nabla} \cdot \nabla) A_i + (1/l^2) A_i (1/-\bar{\nabla} \cdot \nabla) (-\nabla_i \bar{\nabla}_j) A_j + \dots].$$

The purpose of this Letter is to present the full phase diagram of this model in the simplest case for  $\nu=1$  as obtained by Monte Carlo simulations of the partition function  $Z_r = \sum_{\{h, A_i\}} \exp(-\beta E_r)$ , with  $E_r$  taken in the roughening representation of Eq. (3). We apply the standard Metropolis algorithm with trial values for  $h(\mathbf{x})$  and  $A_i(\mathbf{x})$  chosen randomly from one above or one below the current value at each site. Periodic boundary conditions were used. The transition points were found by our measuring first the specific heats, for an estimate, and afterwards the correlation functions, for a precise determination.

The specific heat (per site) is defined as<sup>9</sup>  $C = T^2 \times (\partial^2/\partial T^2) \ln Z_r / L^2$  where  $L^2$  is the number of sites of the square lattice. Using this definition, we can compare directly with the limiting cases for large  $l^2$  (DG model) and small  $l^2$  (LR model) (omitting constant factors and trivial background terms of the Dulong-Petit type). The correlation functions are defined by

$$c^h(x-x') \equiv \frac{1}{2} L \langle [\bar{h}(x) - \bar{h}(x')]^2 \rangle, \quad (5)$$

$$c_i^A(x-x') \equiv \frac{1}{2} L \langle [\bar{A}_i(x) - \bar{A}_i(x')]^2 \rangle, \quad i=1,2,$$

where the angular brackets denote thermal averages with respect to  $Z_r$ , and the bars denote a configuration average along one column; e.g.,  $\bar{h}(x) = L^{-1} \sum_{y=1}^L h(x,y)$ . In  $\mathbf{k}$  space, these averages are equivalent to a projection on the  $k_1$  axis, leading to simple one-dimensional Fourier representations for  $c^h(x)$  and  $c_i^A(x)$  (which, in the free field case, can be evaluated analytically even on finite lattices).

Let us briefly summarize the theoretically expected behavior of these correlation functions, assuming a large enough  $l^2$  to avoid degenerate situations to be discussed later. In the low-temperature solid phase, there are very few defects, and the discrete variables  $h, A_i$  can be treated effectively as massless continuous fields. The dilute gas of bound defects manifests itself only in a renormalization of the temperature, i.e.,  $\beta \rightarrow \beta^R$ , whose effect is exponentially small because of the finite activation energies, i.e., low fugacities. The two-dimensional versions of the correlation functions (5) may then be read off directly from Eq. (4) (if we interpret  $2\pi\theta, 2\pi b_i$  as fixed external sources and replace  $\beta$  by  $\beta^R$ ), yielding

$$c^h(x) = -4\beta^R[(1+\nu)/2] \{G_4(x) + [2l^2/(1+\nu)]G_2^{(0)}(x)\},$$

$$c_1^A(x) = -4\beta^R G_2^{(1/l)}(x), \quad (6)$$

$$c_2^A(x) = -4\beta^R[(1+\nu)/2]G_2^{(0)}(x),$$

where  $G_2^{(m)}$  and  $G_4$  are given by

$$G_2^{(m)}(x) = \frac{1}{L} \sum_{n=1}^{L-1} \frac{e^{ikx} - 1}{2(1 - \cos k) + m^2}, \quad k = \frac{2\pi}{L} n \quad (7)$$

$$G_4(x) = \frac{1}{L} \sum_{n=1}^{L-1} \frac{e^{ikx} - 1}{[2(1 - \cos k)]^2}.$$

Then, with increasing temperature, we expect that the fields  $A$  become effectively massive at some point as a two-dimensional disorder version of the Meissner effect<sup>10</sup> in superconductivity. As a consequence, the  $h$  correlations are screened at long range to

$$c^h(x) = 4\beta^R l^2 G_2^{(0)}(x), \quad (8)$$

which is exactly the behavior in the massless phase of the DG model [with respect to  $h(\mathbf{x})$ ]. Since in this phase the field  $A$  is frozen<sup>9</sup> to an almost uniform constant value, the DG approximation is expected to be excellent, suggesting a second phase transition where the  $h$  correlations also become massive.<sup>7</sup> In the defect picture, this can be interpreted as an unbinding transition of disclination pairs held together by the interaction potential (8) (in the two-dimensional unprojected form which is of the usual Coulomb type).

As long as these transitions are well separated (which is certainly the case for large  $l^2$ ), the standard Kosterlitz-Thouless argument shows that the renormalized stiffness constants  $\beta^R$  have the following universal values: at the first transition  $\beta^R(\beta_c^{(1)}) = 1/\pi - 2/(1+\nu)$ , and at the second transition  $\beta^R(\beta_c^{(2)}) = 1/2\pi l^2$ . Thus, plotting in the low-temperature phase  $c_2^A(x)$  versus  $-G_2^{(0)}(x)$ , we expect a straight line for all  $\beta > \beta_c^{(1)}$  with a limiting minimal slope  $4\beta^R(\beta_c^{(1)}) \times (1+\nu)/2 = (\beta_c^{\text{DGR}})^{-1} = 4/\pi$  at  $\beta_c^{(1)}$ . For  $\beta < \beta_c^{(1)}$ , the correlation length (=inverse mass) is finite, which, in such a plot, is signaled by a downward curvature for large distances. If the lattice size is smaller than this finite correlation length, then the curve still appears straight, but now with a slope smaller than  $4/\pi$ . By a comparative finite-size scaling analysis of the ordinary DG model transition (which appears in the limit  $l \rightarrow \infty$ ), we have checked that this "slope criterion" gives reliable estimates of  $\beta_c$  with practically no finite-size dependence for lattices larger than  $16 \times 16$ .

In this work, we have measured the correlation functions on  $32 \times 32$  lattices using 500 000 configurations for the thermal averages, after discarding 100 000 configurations for equilibration. Using the above slope criterion, we have determined the transition points (for  $\nu=1$ ) shown in the  $l^2$ - $T$  phase diagram of Fig. 1 as open circles. The solid lines are an interpolation of these data.

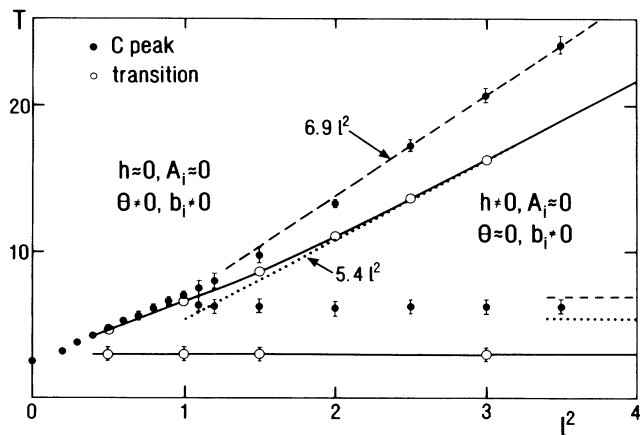


FIG. 1. The phase diagram of the lattice-defect melting model for  $\nu=1$ . The abscissa is the square of the length scale of rotational stiffness, and the ordinate, the temperature. The transition points are determined from measurements of correlation functions on  $32 \times 32$  lattices. In the hot phases we have indicated the roughness of the integer field configurations  $h, A_i$  and the defects as in Ref. 7. The lower phase contains very few defects and is completely rough in  $h$  and  $A_i$ . On the right-hand margin we have indicated the position of the specific-heat peak and the Kosterlitz-Thouless transition for  $l=\infty$ . At finite  $l$ , the transition temperatures are lower by a factor of about 2 since the longitudinal mode has only a finite range  $l$  and does not contribute to the critical limit of the renormalization flow. The peak in the specific heat has only small  $1/l^2$  corrections.

The dotted line with slope 5.4 shows what we would expect in a pure DG model. Since  $T=8\beta^{\text{DG}}l^2$  and from the comparative study  $\beta_c^{\text{DG}}=0.677 \pm 0.010$ , we calculate the slope  $0.677 \times 8 \approx 5.42$ , in excellent agreement with the data. The filled circles show the location of the peaks of the specific heat,  $\beta_{\text{peak}}$ , measured on  $16 \times 16$  lattices. For a few characteristic  $l^2$ , we have plotted the specific-heat curves over a wide temperature range in Fig. 2. To determine the precise location of the maxima, we have performed additional runs near the tip of the peaks with much higher statistics. Furthermore, we have studied the finite-size scaling behavior for  $l^2=0.2, 0.5, 1.0$ , and  $3.0$  (using lattices up to  $64 \times 64$ ) to make sure that there is no significant shift of  $\beta_{\text{peak}}$  on larger lattices. The dashed line with slope 6.9 is the peak position expected from the pure DG model, where the comparative study gave  $\beta_{\text{peak}}^{\text{DG}}=0.861 \pm 0.005$  and thus the slope  $0.861 \times 8 = 6.89$ .

For  $l^2 \gtrsim 2$ , the peak heights depend only weakly on  $L$ , proving that the correlation length  $\xi$  under the peak is finite ( $\xi \approx 3a$ ). The transition points, where the correlation length becomes infinite, lie about 20%–25% below the peaks. This is a clear evidence for two Kosterlitz-Thouless transitions. Around  $l^2 \approx 1$  the two peaks merge into a single one, while we still observe two transitions. The lower one stays almost constant around  $T=3$ . The upper one moves closer and closer to the peak loca-

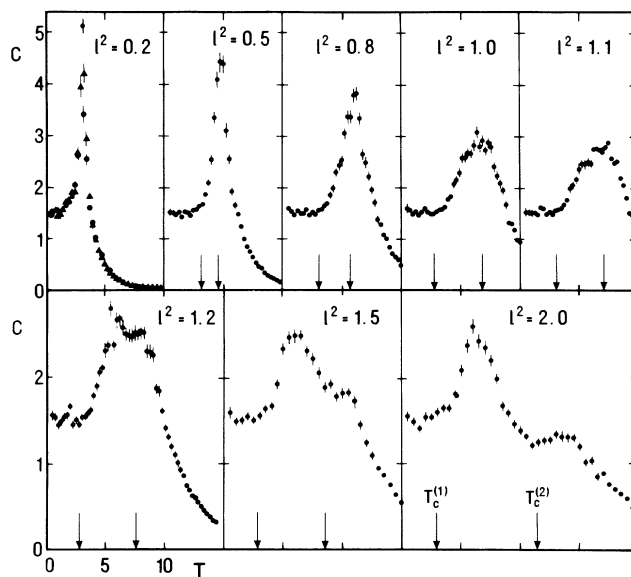


FIG. 2. The specific heat vs temperature of the defect melting model on a  $16 \times 16$  lattice with increasing length scale of rotational stiffness  $l$ . In all plots, the temperature scale is the same. The arrows indicate the transition points which, for  $l^2 > 1$ , lie clearly below the peaks. It is not necessary to plot the peaks for larger  $l^2$  since they follow quite well the appropriately rescaled specific-heat curves of the ordinary DG model. The data are averages over 5000 configurations, after discarding 1000 configurations for thermalization.

tion until around  $l^2 \approx 0.5$  a difference is hardly detectable. Simple extrapolations of these transition lines suggest that they meet around  $l^2 \approx 0.1-0.2$ . Since we know from earlier work<sup>6</sup> that at  $l^2=0$ , there is a single first-order transition at  $T \approx 2.45$  (with an entropy jump of  $\Delta s \approx 0.2$  per site), we expect that the transition remains first order at least up to the separation point around  $l^2 \approx 0.1-0.2$ . For larger  $l^2$ , it is conceivable that the lower transition changes immediately to the Kosterlitz-Thouless type, while the upper one remains first order up to some  $l^2$  between  $\approx 0.2$  and  $\approx 0.5$ . This would explain the very small separation between peak location and transition point. This picture is partly confirmed by our simulations at  $l^2=0.2$ . Here, we observe a clear hysteresis in the energy and a pronounced finite-size scaling of the peak height of the specific heat with increasing  $L$ , indicating indeed a first-order transition (with  $\Delta s$  per site still  $\approx 0.2$ ). On the other hand, at  $l^2=0.5$  we do not observe a reliable hysteresis, and the peak height depends only weakly on  $L$  (up to  $L=32$ ). At this  $l^2$  it is, however, very difficult to disentangle a possible singular part of  $C$  from the large background contributions due to the lower, Kosterlitz-Thouless-type transition (whose specific-heat peak could be just shifted above the second transition).

For simplicity, all calculations have been done at  $\nu=1$  where the  $A$  part of the energy is easiest to handle and

theoretical predictions were available.<sup>7</sup> Since the forces between the defects at large separations maintain their qualitative features also for  $\nu \neq 1$ , we do not expect any dependence of the universality class on  $\nu$ .

In conclusion, we see that the new model of defect melting with a length scale of rotational stiffness is apparently the simplest lattice model rich enough to incorporate the various experimental two-dimensional melting processes.

This work was supported in part by the Deutsche Forschungsgemeinschaft under Grant No. Kl 256.

---

<sup>1</sup>J. M. Kosterlitz and D. J. Thouless, *J. Phys. C* **6**, 1181 (1973), and *Prog. Low Temp. Phys.* **7B**, 371 (1978); J. M. Kosterlitz, *J. Phys. C* **7**, 1046 (1974); D. R. Nelson, *Phys. Rev. B* **18**, 2318 (1979); D. R. Nelson and B. I. Halperin, *Phys. Rev. B* **19**, 2457 (1979); A. P. Young, *Phys. Rev. B* **19**, 1855 (1979).

<sup>2</sup>R. Pindak, D. E. Moncton, S. C. Davey, and J. W. Goodby, *Phys. Rev. Lett.* **46**, 1135 (1981); S. B. Dierker, R. Pindak, and R. B. Meyer, *Phys. Rev. Lett.* **56**, 1819 (1986); J. D. Brock, A. Aharony, R. J. Birgeneau, K. W. Evans-Lutterodt, J. D. Litster, P. M. Horn, G. B. Stephenson, and A. R. Tajbakhsh, *Phys. Rev. Lett.* **57**, 98 (1986); A. Aharony, R. J. Birgeneau, J. D. Brock, and J. D. Litster, *Phys. Rev. Lett.* **57**, 1012 (1986).

<sup>3</sup>M. Bretz, J. G. Dash, D. C. Hickernell, F. O. McLean, and O. E. Vilches, *Phys. Rev. A* **8**, 1589 (1973), and **9**, 2814

(1974) (for <sup>4</sup>He).

<sup>4</sup>J. O. Hansen and L. Verlet, *Phys. Rev.* **184**, 151 (1969); see also L. Verlet, *Phys. Rev.* **159**, 98 (1967); S. Toxvaerd, *J. Chem. Phys.* **69**, 4750 (1978); F. F. Abraham, in *Ordering in Two Dimensions*, edited by S. K. Sinha (North-Holland, Amsterdam, 1980).

<sup>5</sup>P. A. Heiney, R. J. Birgeneau, G. S. Brown, P. M. Horn, D. E. Moncton, and P. W. Stephens, *Phys. Rev. Lett.* **48**, 104 (1982); S. K. Sinha, P. Vora, P. Dutta, and L. Passell, *J. Phys. C* **15**, L275 (1982); J. P. McTague, J. Als-Nielsen, J. Bohr, and M. Nielsen, *Phys. Rev. B* **25**, 7765 (1982) (mainly on Ar).

<sup>6</sup>H. Kleinert, *Phys. Lett.* **91A**, 295 (1982), and **95A**, 381 (1983), and **96A**, 302 (1983); W. Janke and H. Kleinert, *Phys. Lett.* **105A**, 134 (1984), and **114A**, 255 (1986); S. Ami and H. Kleinert, *J. Phys. (Paris), Lett.* **45**, 877 (1984); H. Kleinert, *Phys. Lett.* **97A**, 51 (1983); W. Janke and D. Toussaint, *Phys. Lett. A* **116**, 387 (1986); for a detailed exposition, see the textbook H. Kleinert, *Gauge Theory of Stresses and Defects* (World Scientific, Singapore, 1988). We do not agree with the findings of K. J. Strandburg, S. A. Solla, and G. V. Chester, *Phys. Rev. B* **28**, 2717 (1983); K. J. Strandburg, *Phys. Rev. B* **34**, 3536 (1986); D. A. Bruce, *Mater. Sci. Forum* **4**, 51 (1985); who do not go to large enough lattices to see the characteristic finite-size scaling of the specific-heat peak in a first-order transition.

<sup>7</sup>H. Kleinert, *Phys. Lett. A* **130**, 443 (1988).

<sup>8</sup>D. R. Nelson, *Phys. Rev. B* **26**, 269 (1982).

<sup>9</sup>Note that in the  $h, A_i$  formulation, which is dual to the defect representation the temperature interpretation appears inverted.

<sup>10</sup>H. Kleinert, *Lett. Nuovo Cimento* **34**, 464 (1982).